

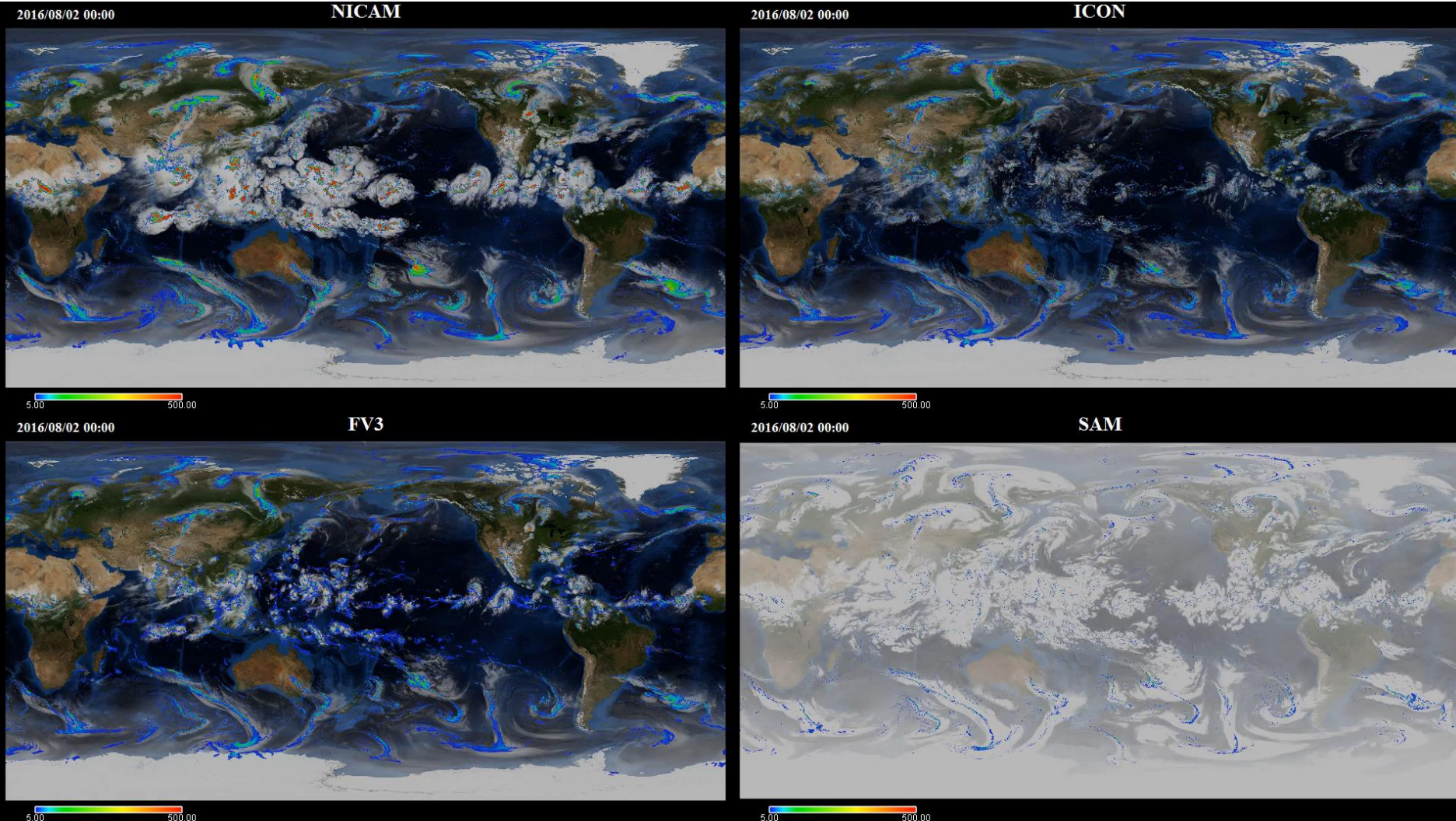
NICAM : Data and Parameterization

Ryosuke Shibuya (Japan Agency for Marine-Earth Science and Technology)

① The information about NICAM

- discretization, parameterization, notes of provided data for DYAMOND...

② Analysis for prediction skills of an intra-seasonal oscillation in DYAMOND models

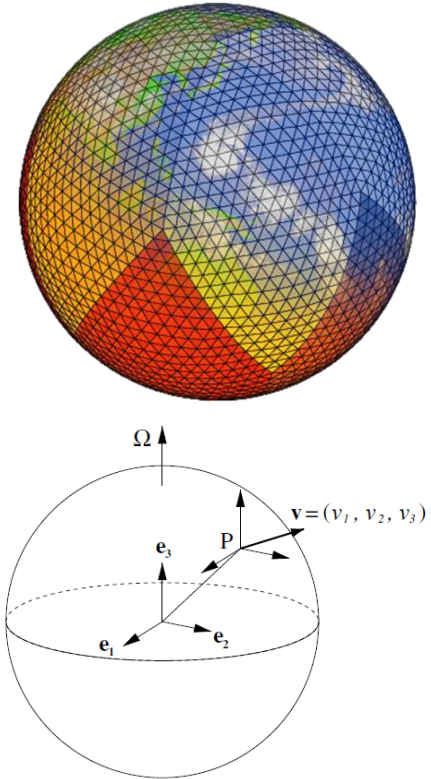


NICAM: Basic equation and numerical method

■ NICAM: **N**on-hydrostatic **I**Cosahedral **A**tmospheric **M**odel

Design of basic equations (Sato et al., 2008):

- Full compressible system
 - solving acoustic wave directly (in the horizontal)
- Flux form
 - finite volume method
- Deep atmosphere
 - including all metrics terms and Coriolis terms
- An orthogonal basis (e_1, e_2, e_3) fixed to the earth
 - avoiding the “pole problem”



$$\frac{\partial \rho}{\partial t} + \nabla \cdot (\rho \mathbf{v}) = 0,$$

$$\frac{\partial \rho \mathbf{v}}{\partial t} + \nabla \cdot (\rho \mathbf{v} \otimes \mathbf{v}) = -\nabla p - \rho g \hat{\mathbf{k}} - 2\rho \boldsymbol{\Omega} \times \mathbf{v}$$

internal energy

$$\frac{\partial \rho e}{\partial t} + \nabla \cdot (h \rho \mathbf{v}) = \mathbf{v} \cdot \nabla p + q_{\text{heat}},$$

$$\frac{\partial (\rho q_d)}{\partial t} + \nabla_h \cdot (\rho q_d \mathbf{v}_h) + \frac{1}{r^2} \frac{\partial (r^2 \rho q_d w)}{\partial z} = s_d,$$

$$\frac{\partial (\rho q_v)}{\partial t} + \nabla_h \cdot (\rho q_v \mathbf{v}_h) + \frac{1}{r^2} \frac{\partial (r^2 \rho q_v w)}{\partial z} = s_v,$$

$$\frac{\partial (\rho q_{1,j})}{\partial t} + \nabla_h \cdot (\rho q_{1,j} \mathbf{v}_h) + \frac{1}{r^2} \frac{\partial [r^2 \rho q_{1,j} (w + w_{1,j}^*)]}{\partial z} = s_{1,j},$$

$$\frac{\partial (\rho q_{i,k})}{\partial t} + \nabla_h \cdot (\rho q_{i,k} \mathbf{v}_h) + \frac{1}{r^2} \frac{\partial [r^2 \rho q_{i,k} (w + w_{i,k}^*)]}{\partial z} = s_{i,k},$$

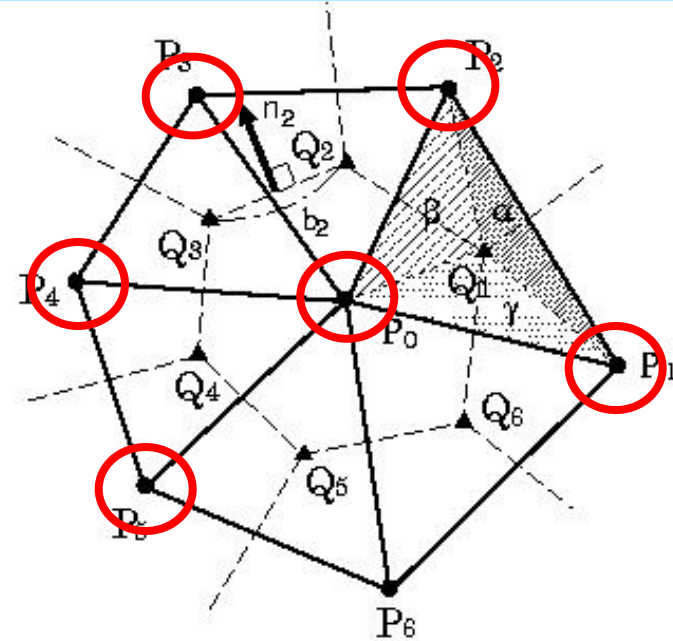
NICAM: Basic equation and numerical method

■ Icosahedral horizontal grid (Tomita and Satoh, 2004)

• Grid system: **Arakawa A-grid**

- all variables at triangular vertices (P_i)
- Hexagonal (pentagonal) control volume

- Easy to implement
- good for parallel computing
- no computational mode
- × non-physical 2-grid scale structure



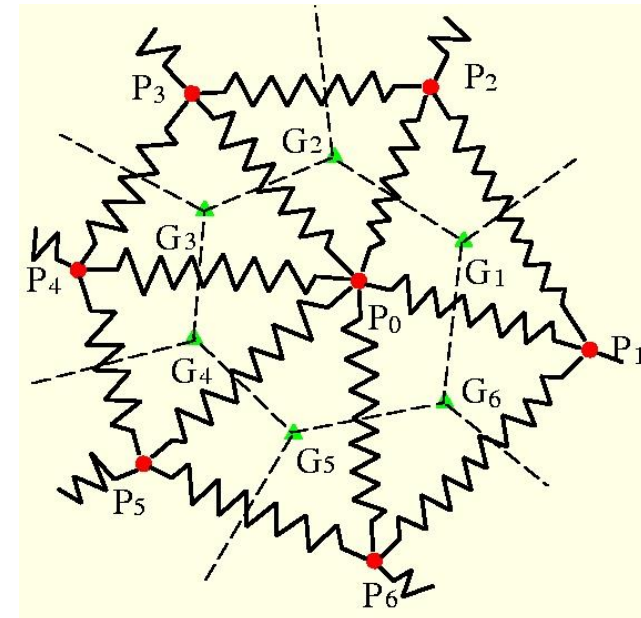
• **Spring dynamics smoothing** (Tomita et al., 2002)

- Triangular vertices (P_i) connected by spring
- solving the spring dynamics
- The system is adjusted to the static balance

$$M \frac{d\mathbf{w}_0}{dt} = \sum_{i=1}^6 k(d_i - \bar{d})\mathbf{e}_i - \alpha\mathbf{w}_0, \quad \frac{d\mathbf{r}_0}{dt} = \mathbf{w}_0$$

• Relocation of grid points to a **gravitational center**

- in a control volume (G_i)
- guarantee the 2nd order accuracy of numerical operator at all of grid points



NICAM: Basic equation and numerical method

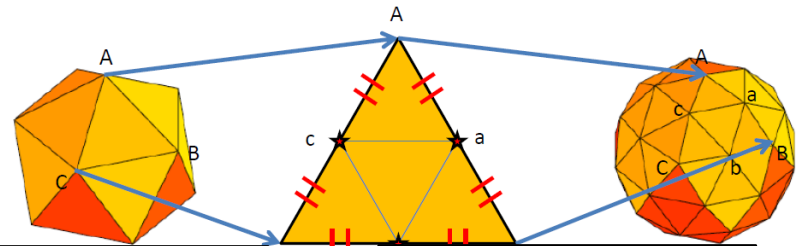
Grid division level (G-level)

- recursive division from the original icosahedron

(a) g-level 0

(b) Grid Division

(c) g-level 1



G-level 9
(dx ~ 14 km):

G-level 10
(dx ~ 7 km):

G-level 11
(dx ~ 3.5 km):

G-level 13
(dx ~ 850 m):

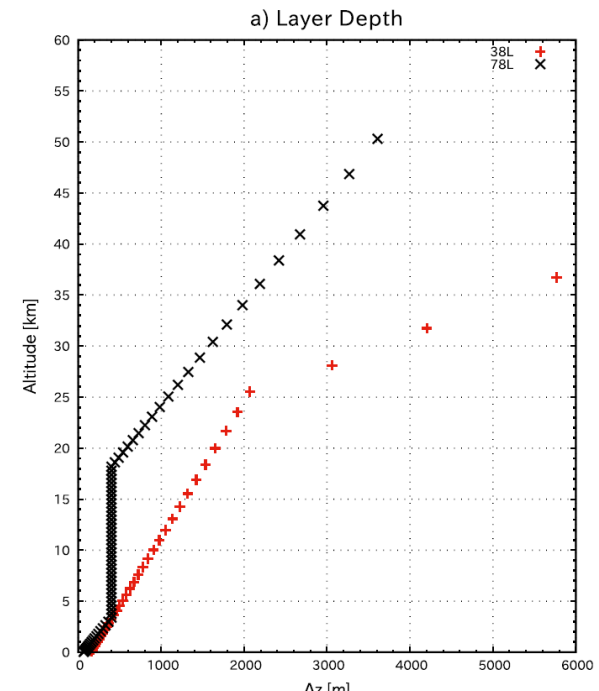
AMIP-type Ex.
kodama et al. (2014)

DYAMOND setting

Sub-km Ex.
Miyamoto et al. (2014)

Vertical grid structure

- L78: dz = 400m below z = 18 km
 - !! Sponge layer is applied above z = 25 km
- Terrain following coordinate
 - !! The topographies in NICAM are smoothed for the stable numerical integration
- Data of the used topography and vegetation have been provided to Mistral



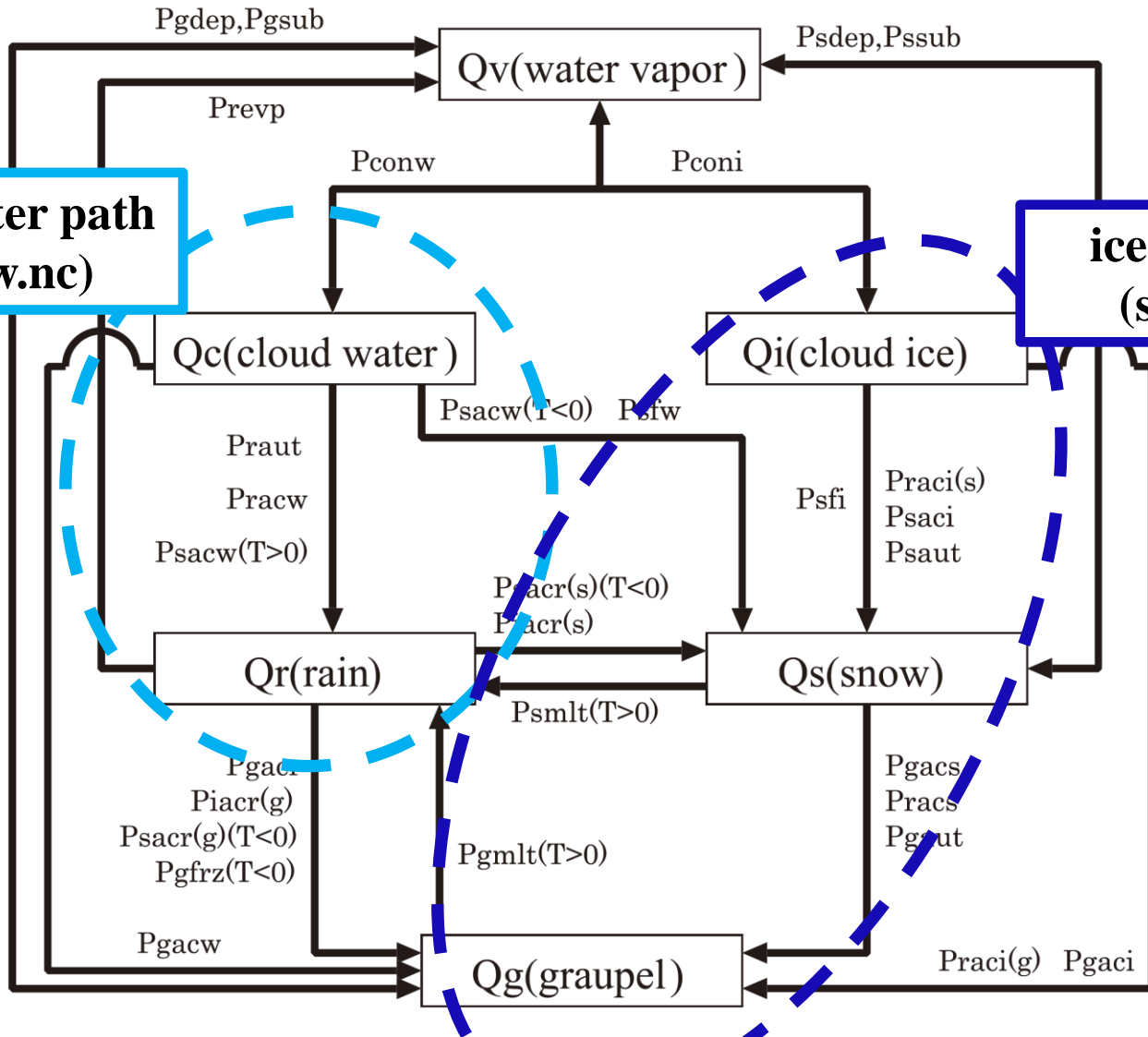
NICAM: physics schemes

	Grid system	microphysics	Radiation	Land-surface
NICAM	Tomita et al., 2008a	Tomita, 2008b; Roh et al., 2017	Sekiguchi and Nakajima, 2008	Takata et al. 2003
ICON	Giorgetta et al., 2018	Doms et al., 2011	Baker et al., 2003	Heise et al., 2006
MPAS	Skamarock et al., 2012	Thompson, 2004	Iacono et al., 2008	Niu et al., 2011
FV3	Putman and Lin, 2007	Chen and Lin, 2013	Anderson et al., 2004	
GEOS5		Bacmeister et al., 2006, etc	Colarco et al., 2010	Koster et al., 2000
SAM	Khairoutdinov and Randall, 2003		Collins et al., 2006	Lee and Khairoutdinov, 2015
	Convective param. (D: deep, S: shallow)	Gravity wave param. (O: orographic, N: non-oro)	Turbulence (T: TKE-type, L: LES-type)	
NICAM	None	None	T: Nakanishi and Niino, 2006	
ICON	None	O: Lott and Miller, 1997 NO: Orr et al., 2010	T: Raschendorfer, 2001 L: Dipankar et al., 2015	
MPAS	D, S: scale-aware Tiedtke (Tiedtke, 1989)	O: Shin et al., 2010	T: Nakanishi and Niino, 2006	
FV3	S: Zhao et al., 2009	O: Lott and Miller, 1997 (as mountain blocking effect)	?	
GEOS5	D: Freitas et al., 2018 S: Bretherton, 2009	O: McFarlane, 1987 NO: Garcia and Boville, 1994	T: Molod et al., 2015	
SAM	None	None	L: Khairoutdinov and Randall, 2003	

SUGGESTION: Let's make a reference table (at DKRZ homepage) in such a format

NICAM: physics schemes

- Microphysics scheme (Tomita, 2008): NSW6 (NICAM Single-moment Water 6)
 - 6 categories for **vapor**, liquid (**cloud water, rain**) and solid (**cloud ice, snow, graupel**)



Liquid water path
(sa_cldw.nc)

ice water path
(sa_cldi.nc)

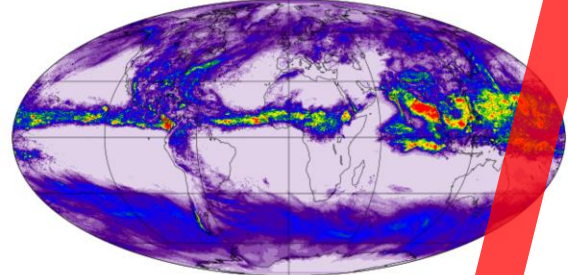
NICAM: physics schemes

• From the 1st DYAMOND Hackathon (thanks to Daniel Klocke)

Solid (**cloud ice, snow, graupel**) water

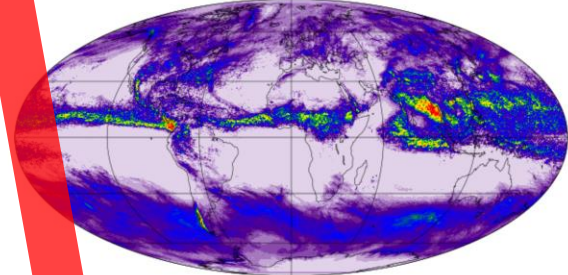


NICAM-3.5km (40 day) TQI [kg/m²] 201608



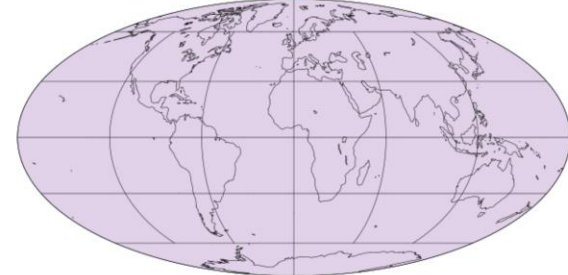
min= 0.000 mean= 0.096 max= 1.416

NICAM-7km (40 day) TQI [kg/m²] 201608



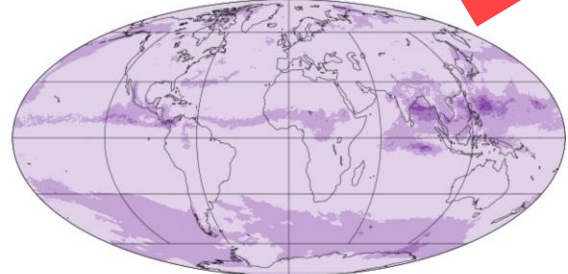
min= 0.000 mean= 0.088 max= 1.030

MPAS-3.75km (40 day) TQI [kg/m²] 201608



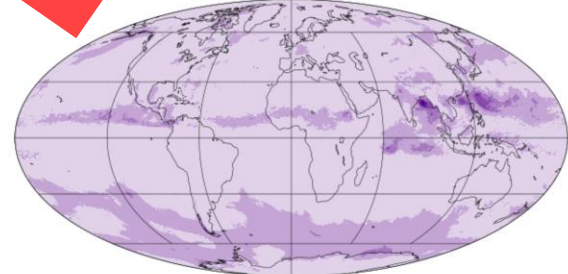
min= 0.000 mean= 0.001 max= 0.014

ICON-2.5km (40 day) TQI [kg/m²] 201608



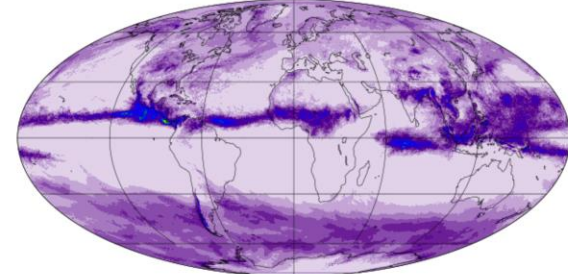
min= 0.000 mean= 0.013 max= 0.092

ICON-5km (40 day) TQI [kg/m²] 201608



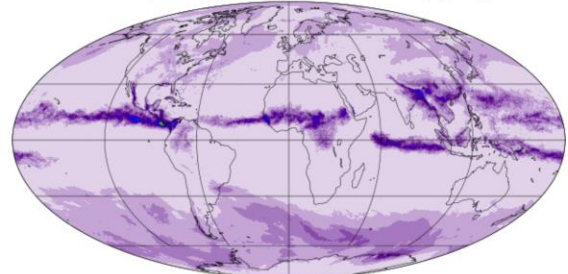
min= 0.000 mean= 0.013 max= 0.126

SAM-4km (40 day) TQI [kg/m²] 201608



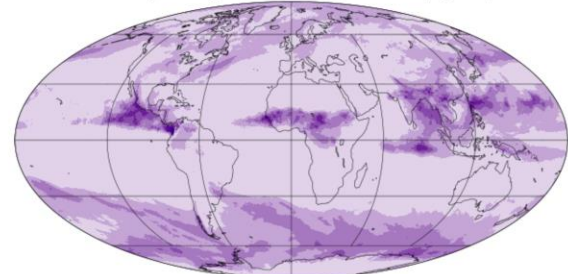
min= 0.000 mean= 0.038 max= 0.549

ECMWF-4km (40 day) TQI [kg/m²] 201608



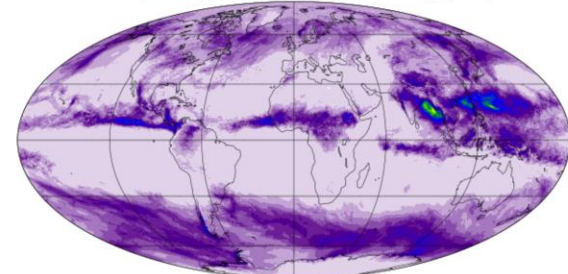
min= 0.000 mean= 0.021 max= 0.579

ECMWF-9km (40 day) TQI [kg/m²] 201608

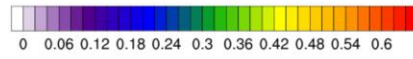


min= -0.000 mean= 0.019 max= 0.186

FV3-3.25km (40 day) TQI [kg/m²] 201608



min= -0.000 mean= 0.041 max= 0.458



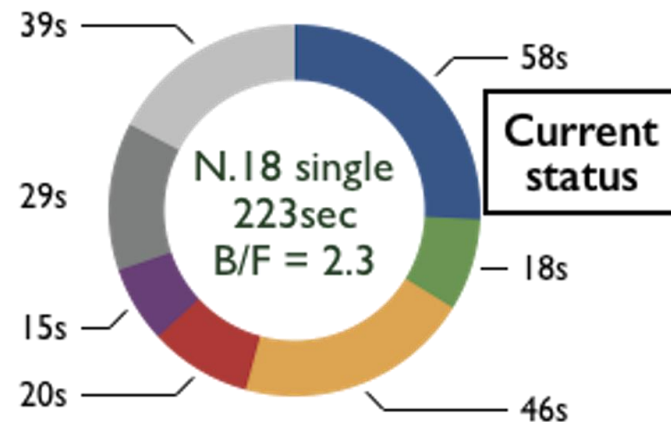
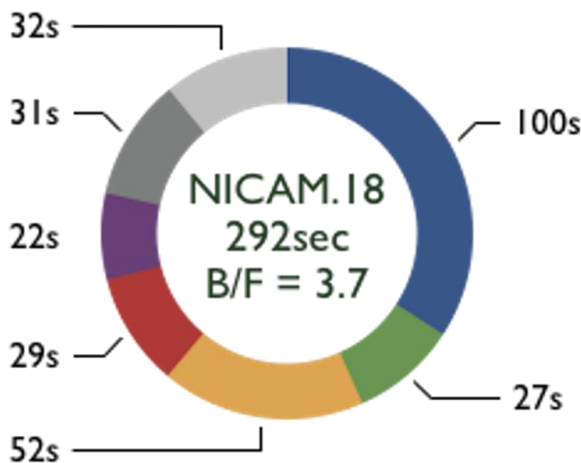
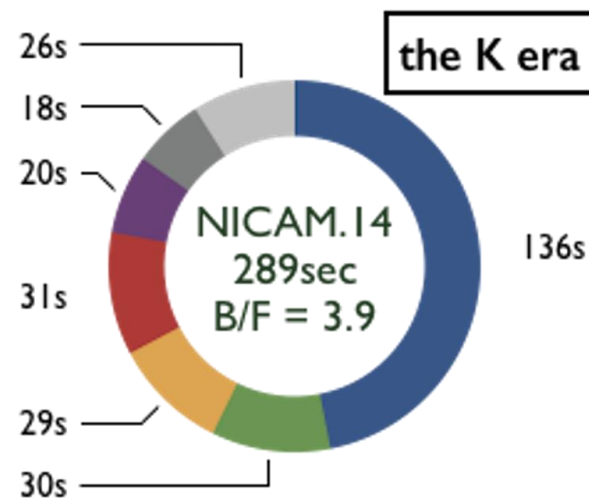
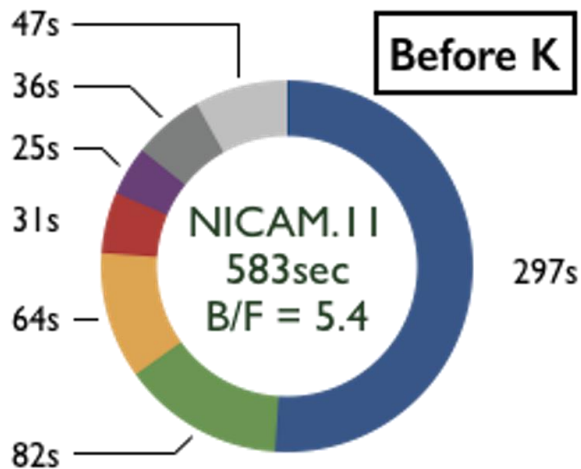
kg/m²

40 day averaged vertical integrated ice

Daniel Klocke

Refactoring/Optimization history on the K computer

- Elapse time of benchmark test (~ GL11, 10 steps) on the K computer.



NICAM: Output variables for DYAMOND

Rule of name: ○(l:land, o:ocean, m:3D atm, s: 2D atm)◎(a:ave, s:snap)_(**variable**)

(Ex; sa_tppn.nc → 2D atm averaged precipitation)

Var	Description	Mistral	Var	Description	Mistral
la_tg	soil temperature	×	oa_ist	sea ice skin temperature	×
la_wg	soil moisture	×	oa_icr	sea ice concentration	×
la_snw	snow amount	×	oa_gflx_adj	Q-flux	×
la_lai	leaf area index	×	dfq_isccp2	ISCCP cloud fraction (ave)	×
la_rof	total runoff	×	ds_isccp2	ISCCP cloud fraction (snap)	×
la_rofl	runoff from each land layer	×	ms_dh	diabatic heating rate	×
la_rofs	runoff by saturation excess	×	ms_u	velocity u	○
la_rofi	runoff by infiltration excess	×	ms_v	velocity v	○
la_rofo	runoff by surface storage overflow	×	ms_w	velocity w	○
la_rofb	runoff from base	×	ms_tem	temperature	○
ls_tg	soil temperature	×	ms_qv	specific humidity	○
ls_wg	soil moisture	×	ms_rh	relative humidity	○
ls_snw	snow amount	×	ms_pres	pressure	○
oa_sst	sea surface temperature	×	ms_qc	specific cloud water content	○
oa_ice	sea ice mass	×	ms_qr	specific rain water content	○
oa_snow	snow on sea ice	×	ms_qi	specific cloud ice content	○

NICAM: Output variables for DYAMOND

変数	Description	Mistral	変数	Description	Mistral
ms_qs	specific snow content	○	ss_tppn	precipitation	○
ms_qg	specific graupel content	○	ss_lwd_toa	downward LW at TOA	○
ms_lwhr	diabatic heating rate by LW	○	ss_lwu_toa	upward LW at TOA	○
ms_swhr	diabatic heating rate by SW	○	ss_lwu_toa_c	upward LW (clear sky) at TOA	○
ms_rh	relative humidity	○	ss_swd_toa	downward SW at TOA	○
sa_cld_frac	cloud fraction	○	ss_swu_toa	upward SW at TOA	○
sa_cldi	ice water path	○	ss_swu_toa_c	upward SW (clear sky)at TOA	○
sa_cldw	liquid water path	○	ss_lwd_sfc	downward LW at the surface	○
sa_evap	evaporation	○	ss_lwu_sfc	upward LW at the surface	○
sa_slp	mean sea level pressure	○	ss_swd_sfc	downward SW at the surface	○
sa_slp_ecmwf	mean sea level pressure formulated by ECMWF	×	ss_swu_sfc	upward SW at the surface	×
ss_q2m	specific humidity at 2m	○	ss_lwd_sfc_c	downward LW (clear sky) at the surface	○
ss_t2m	temperature at 2m	○	ss_lwu_sfc_c	upward LW (clear sky) at the surface	○
ss_tem_atm	mass weighted atmospheric temperature	×	ss_swd_sfc_c	downward SW (clear sky) at the surface	○
ss_tem_sfc	skin temperature	○	ss_swu_sfc_c	upward SW (clear sky) at the surface	○
ss_u10m	velocity u at 10m	○			
ss_v10m	velocity v at 10m	○			
ss_vap_atm	precipitable water	○			

NICAM: Output variables for DYAMOND

Var	Description	Mistral	Var	Description	Mistral
ss_lh_sfc	latent heat flux	○	sa_tauu	surface stress in the longitudinal direction	×
ss_sh_sfc	sensible heat flux	○	sa_tauv	surface stress in the latitudinal direction	×
ss_tppn_energy	other energy flux due to precipitation	○	ms_omg_p3	Vertical velocity (Pa/s) at 850, 700, 500 hPa	×
ss_evap_energy	other energy flux due to evaporation	○	ms_rh_p3	Relative humidity at 850, 700, 500 hPa	×
ss_albedo	surface albedo (inc. scattering)	○			

- Output interval: **3 h** for 3D variables and **15 min** for 2D variables, **CDO is ok**.
- Outputs are already converted from the icosahedral data to separated lat-lon netcdf
- Both “averaged” and “snapshot” outputs would be available for 2D variables
- Missing variables (at 2019/6/17 on Mistral):
 - sa_tauu, sa_tauv (surface wind stress), ss_swu_sfc (upward SW radiation at surface)
 - ms_omg_p3, ms_rh_p3 (omega (Pa/s), relative humidity at 850, 700, 500 hPa)
- CAPE, SIN is not in the output list

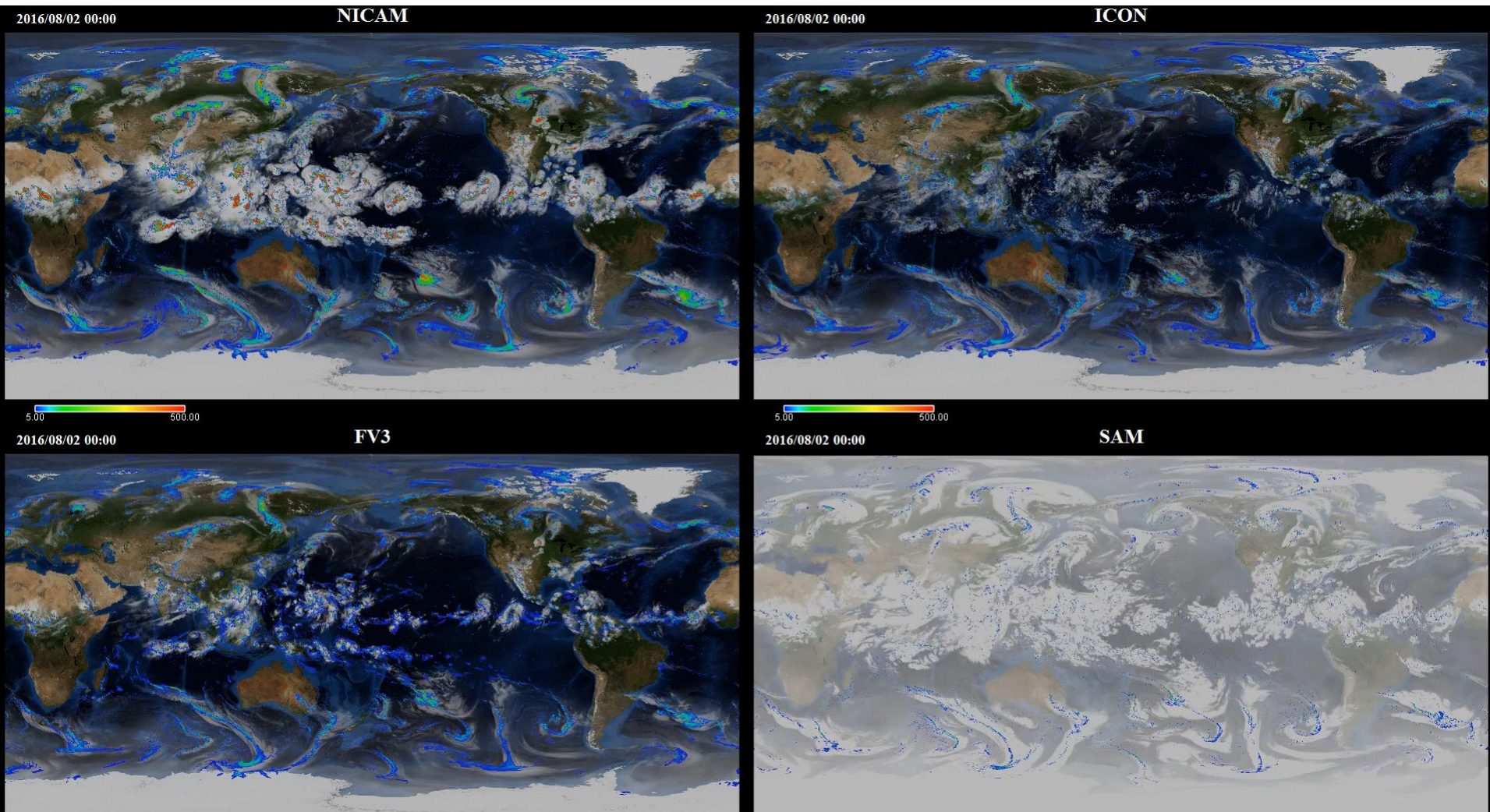
■ In 3.5 km NICAM simulation, a severe initial shock is found for the first two days
 — too large precipitation at 1st and 2nd August, 2016

- When taking an average, please exclude the first two days...

- A new simulation of 3.5 km experiment without the initial shock has been completed
 — the new data will be transported to Mistral until July at the latest

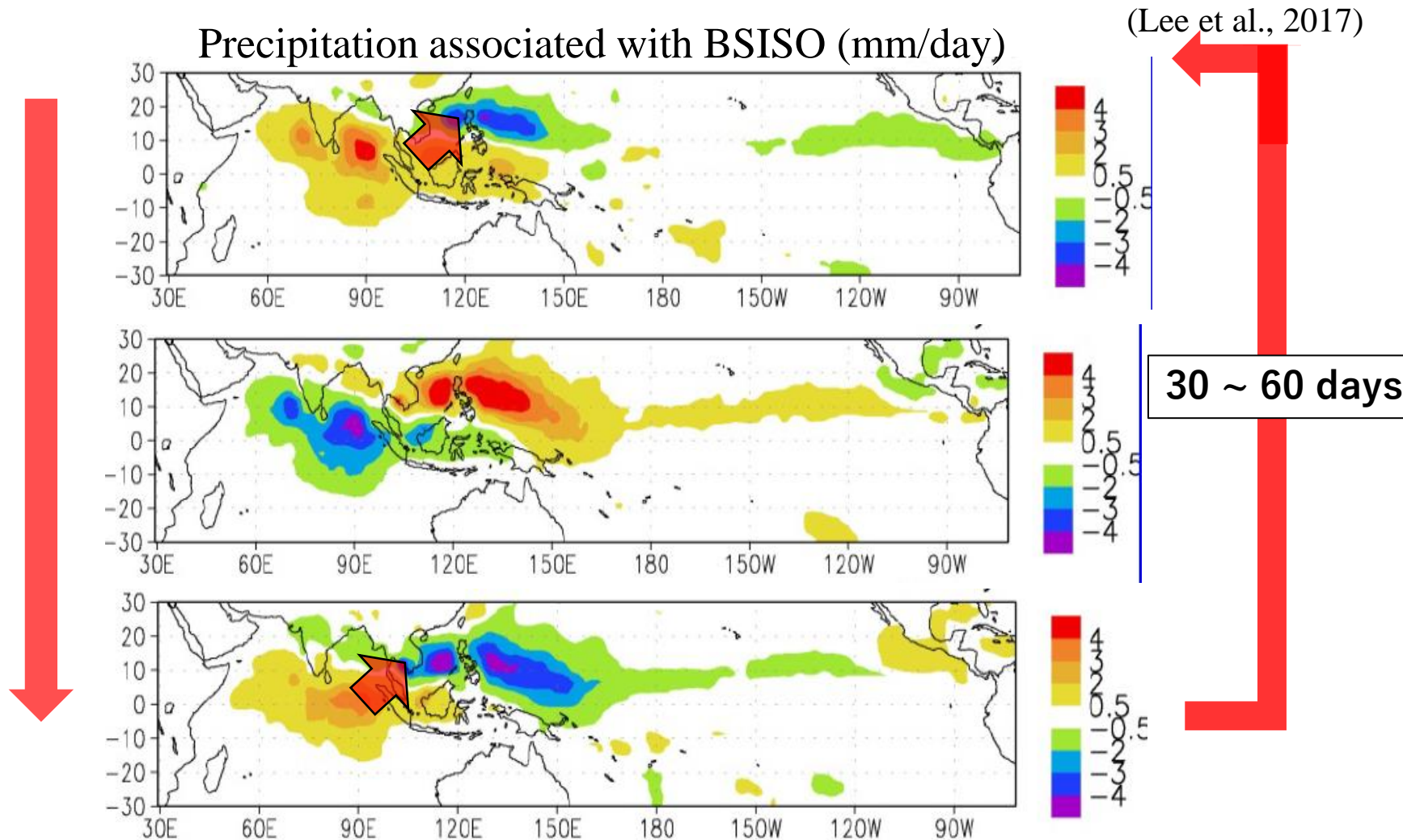
NICAM: Output variables for DYAMOND

- Although a severe initial shock is found in NICAM 3.5 km simulation, a tropical cyclone “OMAIS” is successfully simulated as a hindcast experiment (So the simulation itself is likely not broken even in the 1st experiment...)



The Boreal Summer Intra-Seasonal Oscillation

- Tropical intra-seasonal oscillation (ISO) has a significant amplitude (**BSISO**)
 - characterized by northwest-southeastward tilted rain band (e.g., Yasunari 1979)
- It is suggested that BSISO is a source of **an intra-seasonal predictability**
 - possibly leading to that of teleconnection pattern in the Asian region



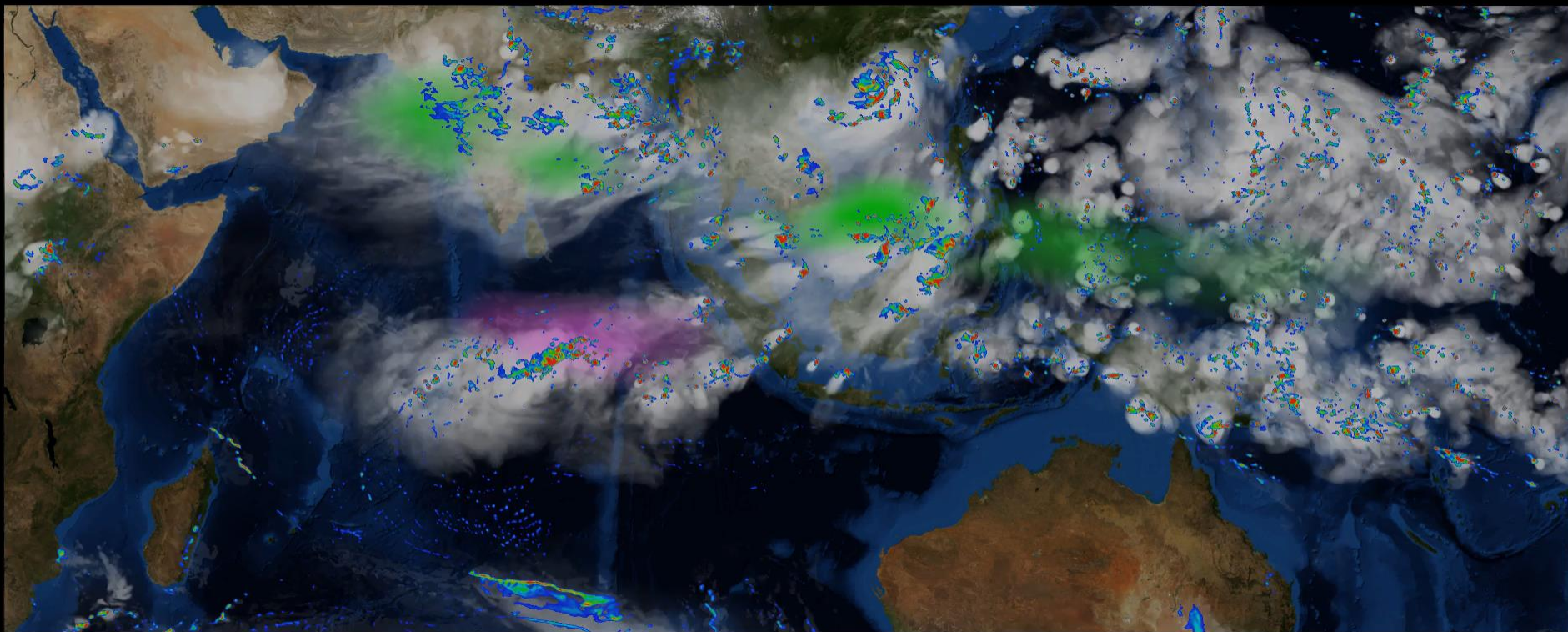
The Boreal Summer Intra-seasonal Oscillation

- In the DYAMOND period, the BSISO **with a relatively large amplitude** occurred
 - A good target for the DYAMOND project as a hindcast experiment
 - It is valuable to clarify forecast skills of the BSISO by DYAMOND models

NICAM 7 km,
white (raw OLR), green/pink (negative/positive intra-seasonal scale OLR)

2016/08/02 00:00

NICAM



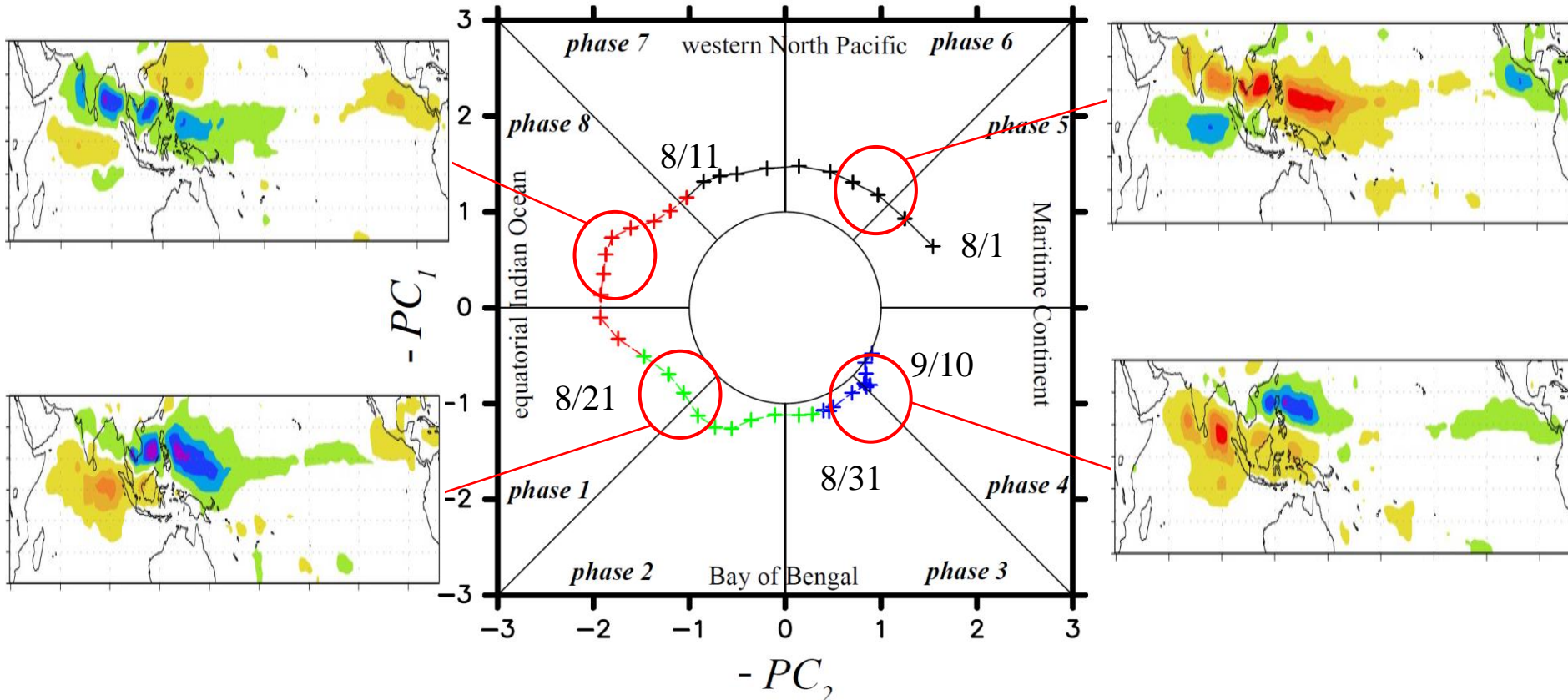
Representation by a BSISO Index (Kikuchi et al., 2012)

○ Assumption:

The BSISO mode is constructed by the 1st and 2nd mode of OLR fields in EEOF in JJA from 1979 to 2009, with lags of -10, -5, and 0 days

⇒ the time/special structure of the BSISO can be represented by **PC₁ and PC₂**

■ Time-evolution of BSISO by CERES from 1st August 2016 ~ 10th September 2016



○ Good point: Intuitive understanding, applicable for an evaluation of forecast skills

Evaluation of Forecast skill score (Matsueda and Endo, 211)

- (PC_1, PC_2) is obtained by projecting simulated/observed seasonal-filtered OLR field to EEOF1,2
- Bivariate correlation (COR):
 - Cosine of an angle between (PC_1, PC_2) of the observation and a model on the phase space (COR of 1.0 means perfect prediction except for amplitude)

$$\begin{aligned} COR^i(t, \tau) &= \frac{a_1(t)f_1^i(t, \tau) + a_2(t)f_2^i(t, \tau)}{\sqrt{a_1(t)^2 + a_2(t)^2} \sqrt{f_1^i(t, \tau)^2 + f_2^i(t, \tau)^2}} \\ &= \cos \vartheta \end{aligned}$$

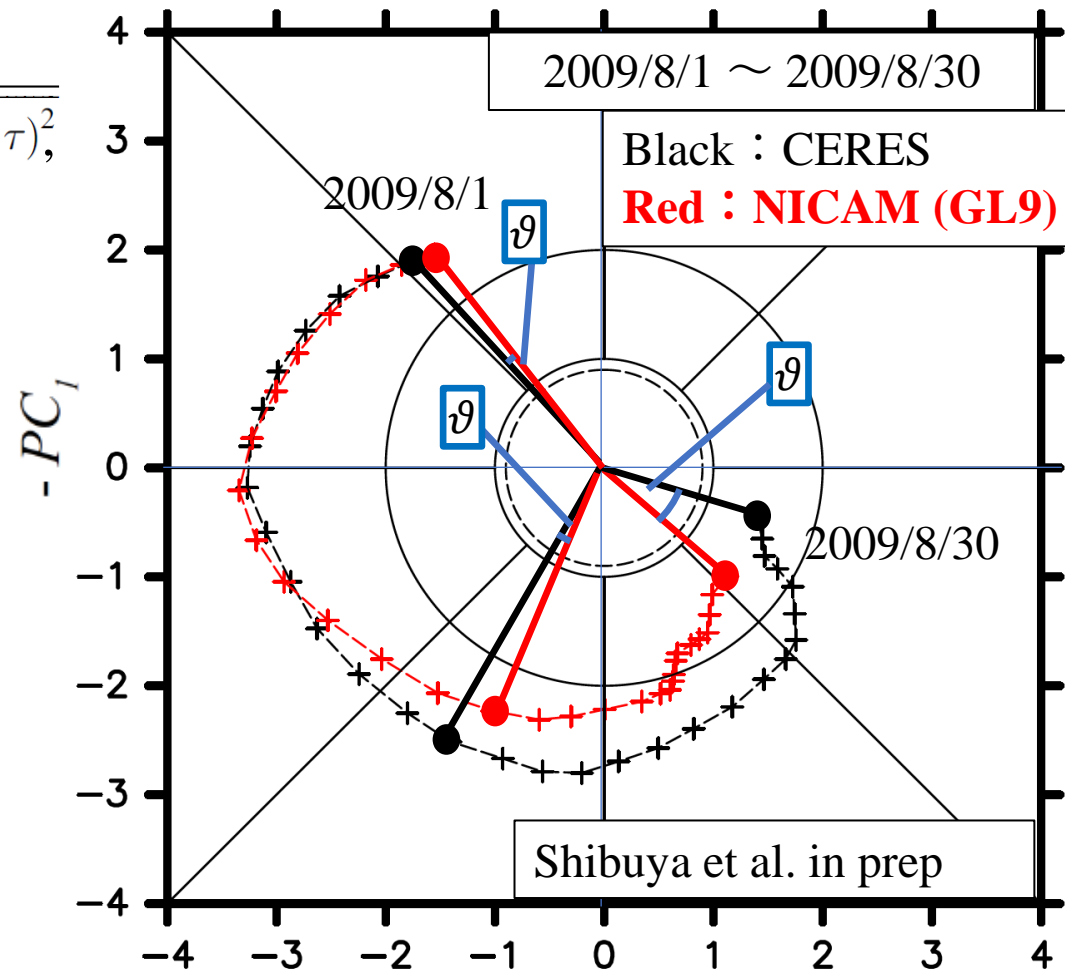
A threshold for “prediction skill”

- $COR > 0.6$ (or, 0.5)
- correspond to an angle of about 50° on the phase space

• Example:

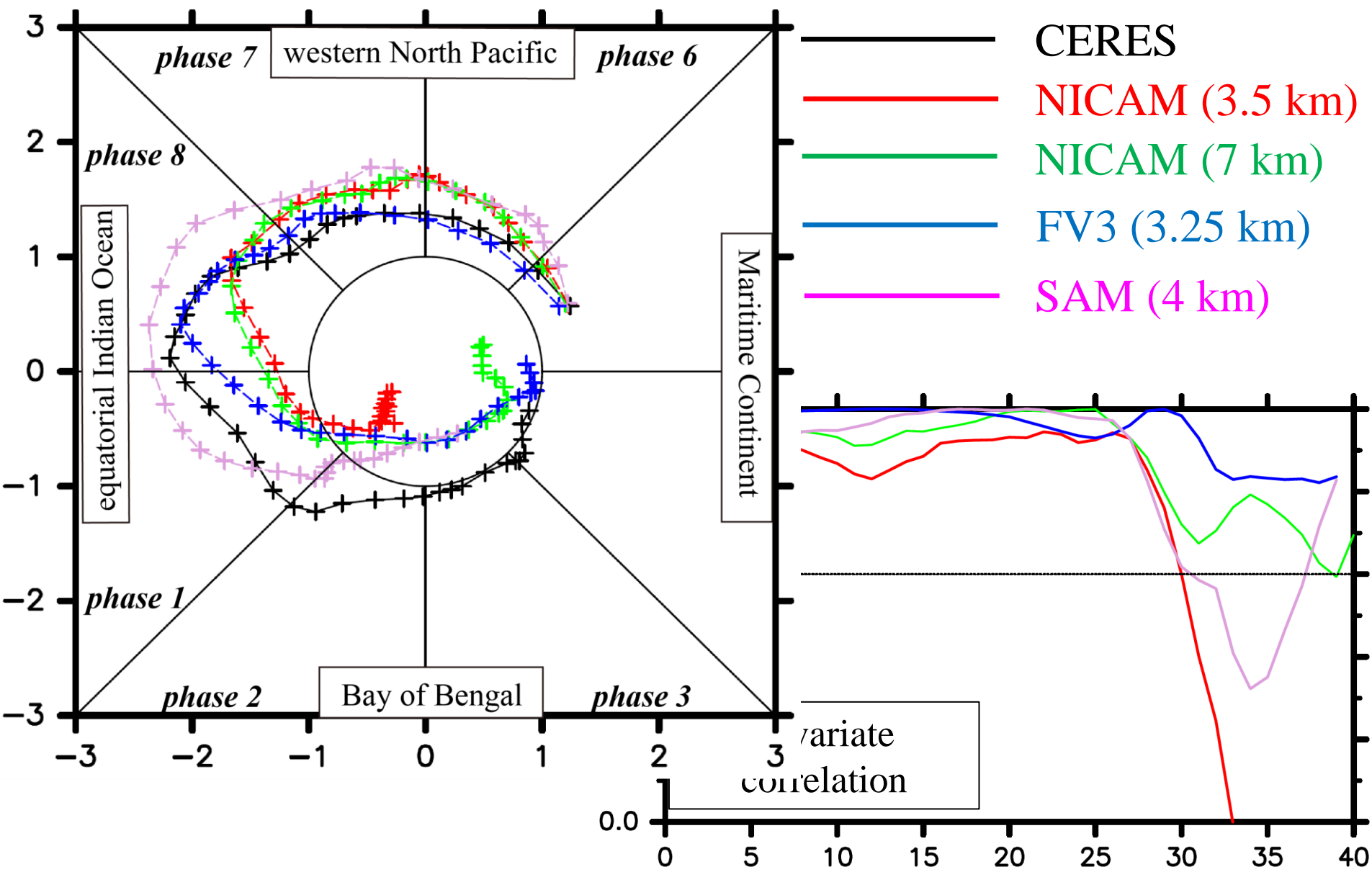
A hindcast experiment by GL9
(14 km NICAM)

- In this case,
COR~0.87 on 2019/8/30



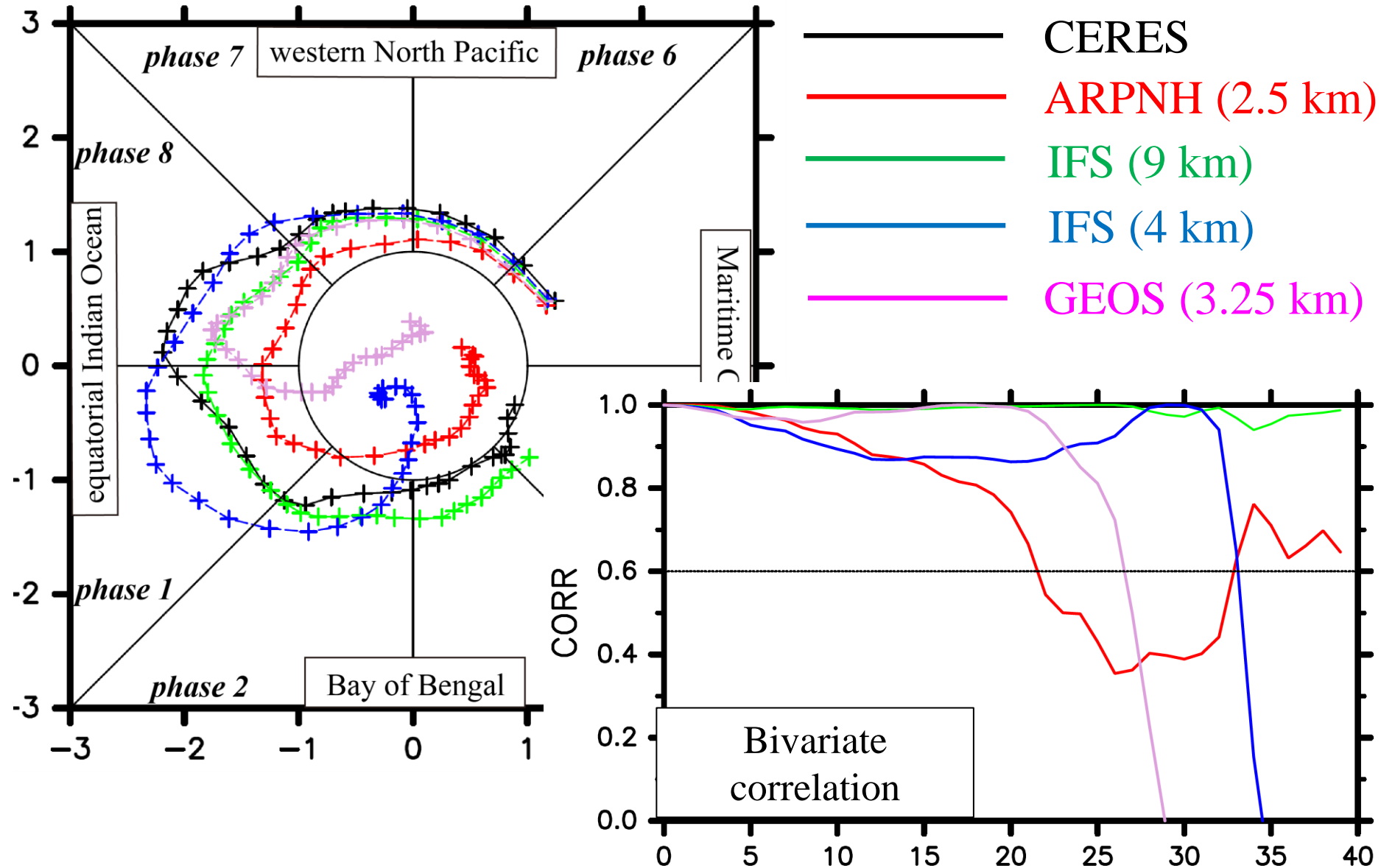
Forecast scores for **NICAM (3.5 km, 7 km), FV3, SAM**

- The forecast scores for DYAMOND models are evaluated by their OLR on Mistral



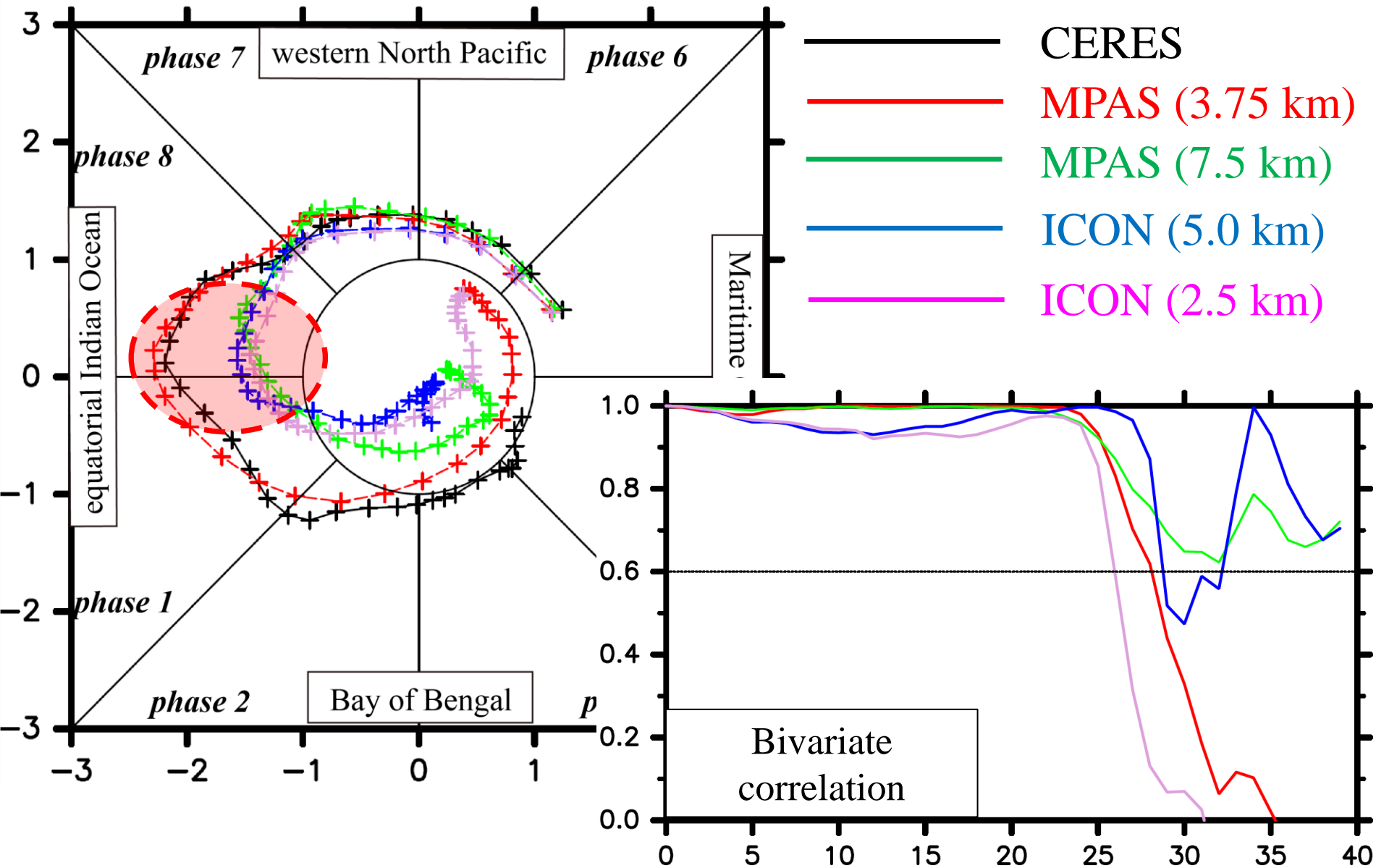
Forecast scores for **ARPNH, IFS (9km, 4km), GEOS**

- The forecast scores for DYAMOND models are evaluated by their OLR on Mistral



Forecast scores for **MPAS (3.75, 7.5 km)**, **ICON (5.0, 2.5km)**

- The forecast scores for DYAMOND models are evaluated by their OLR on Mistral



Analysis plan for understanding the model biases

- The forecast scores for DYAMOND models based on COR



IFS-9 km



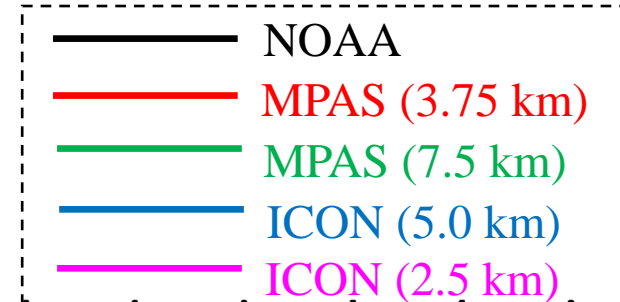
FV3



MPAS-7.5 km, NICAM-7 km

— **Forecast skill over 4 weeks in the ensemble is surprisingly good!!**

— indicating the advantage of high-resolution global models for the forecast of BSISO

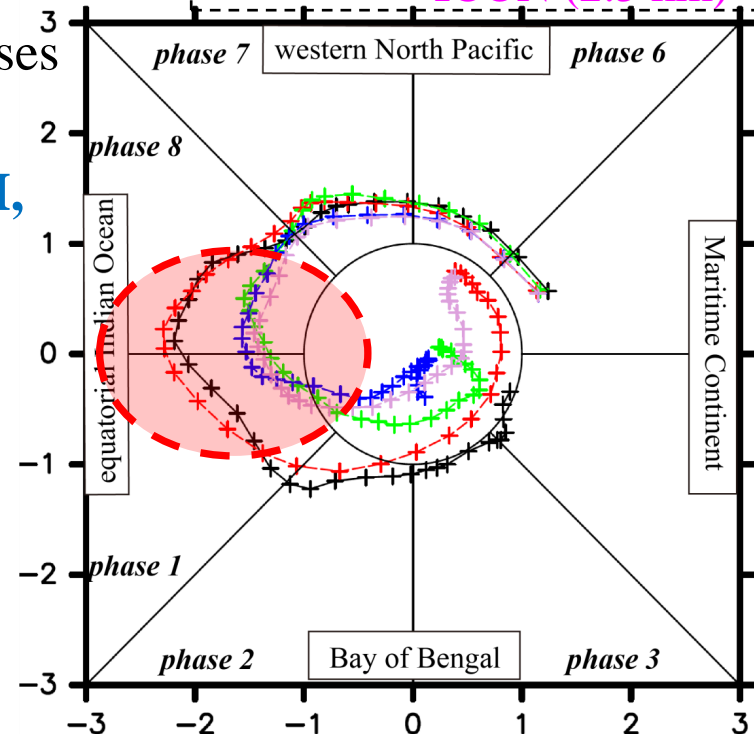


■ The DYAMOND models have similar BSISO biases

- Too small amplitude** from phase 8 to phase 1 (NICAM 3.5km, 7km, FV3, GEOS, ARPNH, MPAS 7.5km, ICON 2.5km, 5km)

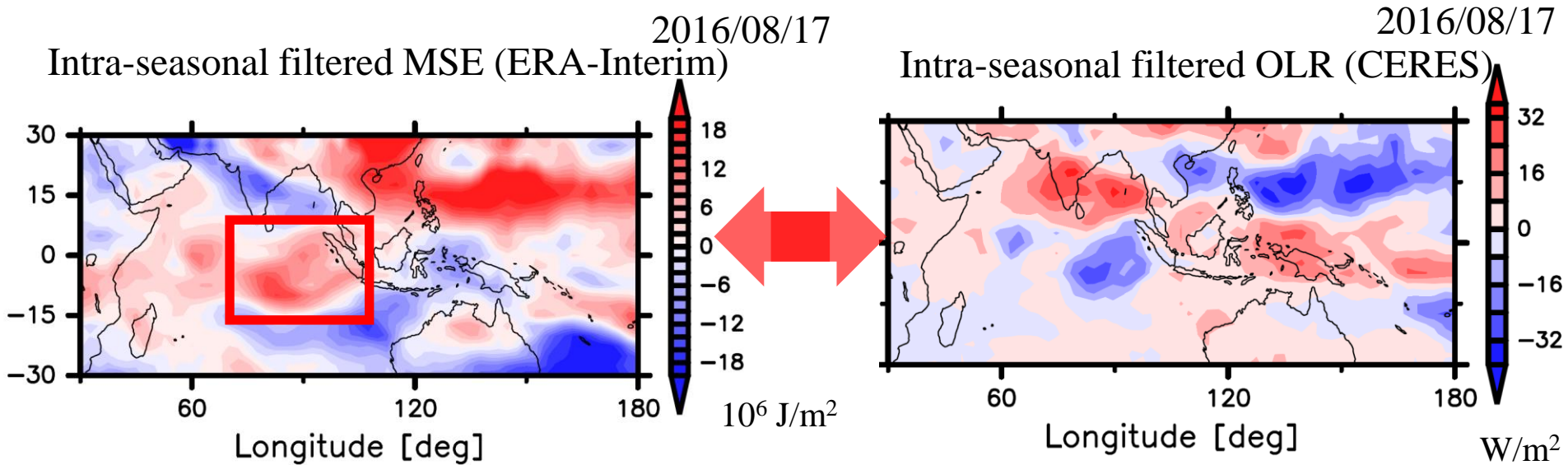
— corresponding to the underestimation of a re-initiation process of convection over the Indian Ocean

- Too fast propagation** of BSISO (ARPNH, IFS 9km, ICON 2.5km, 5km)



Analysis plan for understanding the model biases

■ Budget analysis for the column-integrated moist static energy (MSE)



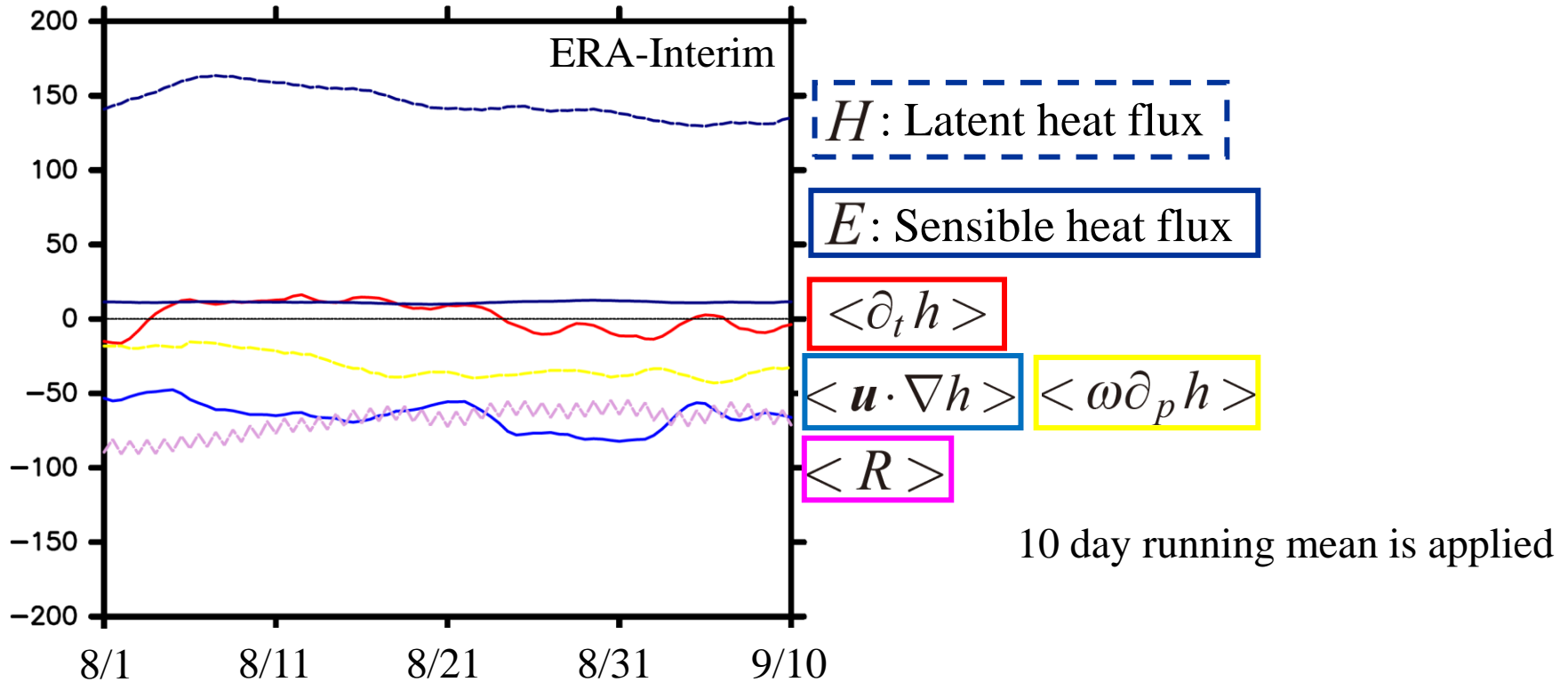
$$\begin{aligned} \langle \partial_t h \rangle + \langle \mathbf{u} \cdot \nabla h \rangle + \langle \omega \partial_p h \rangle \\ = \langle R \rangle + E + H \equiv \langle Q_1 - Q_2 \rangle, \end{aligned}$$

$$\langle (\cdot) \rangle \equiv \frac{1}{g} \int_{p_t}^{p_s} (\cdot) dp, \quad \text{where } h = C_p T + gz + Lq$$

- The contribution for the time-evolution of BSISO by each term will be revealed by evaluating the time-tendency of budget terms of MSE (Sobel & Malony 2012, Yokoi & Sobel, 2015)
- The targeted area \Rightarrow Over the Indian Ocean (0N – 10S, 75-100)

Analysis plan for understanding the model biases

- Time-evolution of each term in the MSE equation (ERA-Interim) over the target area during 1st August 2016 ~ 10th September 2016

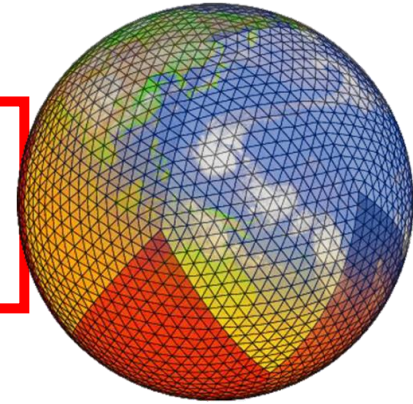


- Regression analysis on $\langle h \rangle$ and $\langle \partial_t h \rangle$ can reveal what process is responsible for **the maintenance of the BSISO amplitude** and **phase propagation** (not shown)
- The budget analysis using DYAMOND data
 - ⇒ obtaining the suggestion for underestimation/slow propagation of BSISO in the DYAMOND models

Summary

- The information about NICAM is described in the former part
 - discretization, parameterization, notes for provided data in DYAMOND
 - Please see Satoh et al. (2008, 2014, 2017) for further detail

- A severe initial shock bias in 3.5 km NICAM at 1st and 2nd August
- A new simulation of 3.5 km experiment has been completed
 - the new data will be transported until July at the latest



- The BSISO with a large amplitude occurred during the DYAMOND period
 - **All of the models show quite good prediction score**
 - ⇒ **over 4 weeks as the ensemble of the DYAMOND models**
 - indicating the advantage of high-resolution global models for the forecast of BSISO
 - Systematic errors for the simulation of BSISO are confirmed
 - the under estimation of BSISO over the Indian Ocean, slow propagation
 - ⇒ This is further examined by evaluating the MSE budget analysis